Gaussian wave packet transform based numerical scheme for the semi-classical Schrödinger equation with random inputs *

Shi Jin[†], Liu Liu[‡], Giovanni Russo[§] and Zhennan Zhou[¶]

March 14, 2019

Abstract

In this work, we study the semi-classical limit of the Schrödinger equation with random inputs, and show that the semi-classical Schrödinger equation produces $O(\varepsilon)$ oscillations in the random variable space. With the Gaussian wave packet transform, the original Schrödinger equation is mapped to an ODE system for the wave packet parameters coupled with a PDE for the quantity w in rescaled variables. Further, we show that the w equation does not produce ε dependent oscillations, and thus it is more amenable for numerical simulations. We propose multi-level sampling strategy in implementing the Gaussian wave packet transform, where in the most costly part, i.e. simulating the w equation, it is sufficient to use ε independent samples. We also provide extensive numerical tests as well as meaningful numerical experiments to justify the properties of the numerical algorithm, and hopefully shed light on possible future directions.

1   Introduction

In simulating physical systems, which are often modeled by differential equations, there are inevitably modeling errors, imprecise measurements of the initial data or the background coefficients, which may bring about uncertainties to the equation. There has been a growing

interest in analyzing such models to understand the impact of these uncertainties, and thus design efficient numerical methods.

When it comes to quantum dynamics, quantifying the effect of uncertainty is even a trickier task. The solution to the Schrödinger equation is a complex valued wave function, whose nonlinear transforms (e.g. position density, flux density) lead to probabilistic measures of the physical observables. Thus, the uncertainty in the Schrödinger equation may or may not result in changes in measurable quantities from the quantum state.

We consider the following semi-classical Schrödinger equation with random inputs

$$i\varepsilon\partial_t\psi^\varepsilon(t,\mathbf{x},\mathbf{z}) = -\frac{\varepsilon^2}{2}\Delta_\mathbf{x}\psi^\varepsilon(t,\mathbf{x},\mathbf{z}) + V(\mathbf{x},\mathbf{z})\psi^\varepsilon(t,\mathbf{x},\mathbf{z}), \qquad (1.1)$$

$$\psi^\varepsilon(0,\mathbf{x},\mathbf{z}) = \psi_{\text{in}}^\varepsilon(\mathbf{x},\mathbf{z}). \qquad (1.2)$$

Here, $\varepsilon \ll 1$ is the semi-classical parameter, which is reminiscent of the scaled Plank constant, and $V(\mathbf{x},\mathbf{z})$ is the scalar potential function, which is slow-varying and often used to model the external field. The initial condition $\psi_{\text{in}}^\varepsilon(\mathbf{x},\mathbf{z})$ will be assumed to be in the form of a semi-classical wave packet, which is a Gaussian wave packet parameterized by the wave packet position, the wave packet momentum, etc.

The uncertainty is described by the random variable $\mathbf{z}$, which lies in the random space $I_\mathbf{z}$ with a probability measure $\pi(\mathbf{z})d\mathbf{z}$. We introduce the notation for the expected value of $f(\mathbf{z})$ in the random variable $\mathbf{z}$,

$$\langle f \rangle_{\pi(\mathbf{z})} = \int f(\mathbf{z})\pi(\mathbf{z})d\mathbf{z}. \qquad (1.3)$$

In this paper, we only consider the uncertainty coming from initial data and potential functions, that is the uncertainty is *classical*. For example, the external classical field, the wave packet position or the wave packet momentum is uncertain, which reflects on the uncertainty in physical observables.

We do not, however, aim to analyze different types of uncertainties in quantum dynamics, but rather, we study how the uncertainty propagates in the semi-classical Schrödinger equation. When $\varepsilon \ll 1$, it is well known that the Schrödinger equation is in the high frequency regime, where the solution generates $O(\varepsilon)$ scaled oscillations in space and time. As we shall show in this paper, the solution generically propagates $O(\varepsilon)$ scaled oscillations in the $\mathbf{z}$ variable as well even if the random variable $\mathbf{z}$ obeys an ε independent probability distribution. The high frequency of the solution in space, time and uncertainty leads to unaffordable computational cost, which makes conventional numerical methods infeasible. Thus, it is of great interest to design efficient numerical method based on the multiscale nature of the analytical solutions.

In the semi-classical regime, due to the $O(\varepsilon)$ scaled oscillation in the solution to the Schrödinger equation, the wave function ψ^ε does not converge in the strong sense as $\varepsilon \to 0$. The high frequency nature of the wave function of the semi-classical Schrödinger equation also causes significant computation burdens. If one aims for direct simulation of the wave function, one of the best choices is the time splitting spectral method, as analyzed in [2] by Bao, Jin and Markowich. See also [10, 12, 21, 3], where the meshing strategy $\Delta t = O(\varepsilon)$

and $\Delta x = O(\varepsilon)$ is sufficient for moderate values of ε. Another advantage of the time splitting methods is that if one is only interested in the physical observables, the time step size can be relaxed to $o(1)$, in other words, independently of ε, whereas one still needs to resolve the spatial oscillations. As we shall show in the paper, when the uncertainty is present, the wave function is also highly oscillatory in the **z** variable, which means the size of samples in random variable grows as $\varepsilon \to 0$ in order to obtain accurate approximations of the quantum dynamics.

There are quite a few approximate methods other than directly simulating the semi-classical Schrödinger equation, which are valid in the limit $\varepsilon \to 0$, such as the level set method and the moment closure method based on the WKB analysis and the Wigner transform, see, for example, [10] for a general discussion. In the past few years, many wave packets based methods have been introduced, which reduce the full quantum dynamics to Gaussian wave packets dynamics [9, 16, 8], and thus gain significant savings in computation cost, such as the Gaussian beam method [25, 11, 24], the Hagedorn wave packet approach [5, 31] and the Frozen Gaussian beam method [13, 14, 18, 20, 19]. When random inputs are considered, in theory, one can design numerical methods based on those approximation tools with ε independent samples in **z**, however, the approximation errors persist in spite of other potential challenges.

A related work to our current subject is [4], where the authors developed the generalized polynomial chaos (gPC)-based stochastic Galerkin method for a class of highly oscillatory transport equations containing uncertainties that arise in semi-classical modeling of non-adiabatic quantum dynamics. Built upon and modified from the nonlinear geometrical optics based method, this scheme can capture oscillations with frequency-independent time step, mesh size as well as degree of the polynomial.

Clearly, an exact reformulation of the semi-classical Schrödinger equation that separates the multiscales in dynamics is desired for efficient simulation. Very recently, Russo and Smereka proposed a new method based on the so-called Gaussian wave packet transform [26, 27, 32], which reduces the quantum dynamics to Gaussian wave packet dynamics together with the time evolution of a rescaled quantity w, which satisfies another equation of the Schrödinger type, in which the modified potential becomes time dependent. We emphasize that the Gaussian wave packet transform is an equivalent reformulation of the full quantum dynamics, and there are no more ε dependent oscillations in the w equation. This motivates us to investigate whether this transform facilitates design of efficient numerical methods for semi-classical Schrödinger equations with random inputs.

In this work, we study the semi-classical limit of the Schrödinger equation with random inputs, which is the Liouville equation with a random force field, and show that the semi-classical Schrödinger equation produces $O(\varepsilon)$ oscillations in the **z** variable in general. However, with the Gaussian wave packet transform, the original Schrödinger equation is mapped to an ODE system for the wave packet parameters coupled with a PDE for the quantity w in rescaled variables, where the ODE system and the w equation also depend on the random variable. Further, we show that the w equation does not produce ε dependent oscillations in the rescaled spatial variable, thus it is more amenable for numerical simulations. We propose multi-level sampling strategy in implementing the Gaussian wave

3

packet transform, where in the most costly part, simulating the w equation, it is sufficient to use ε independent samples, thus the complexity of the whole algorithm has satisfactory scaling behavior as ε goes to 0. We also provide extensive numerical tests as well as meaningful numerical experiments to justify the properties of the numerical algorithm as well as hopefully shed light on possible future directions.

The rest of the paper is outlined as follows. Section 2 discusses the semi-classical limit of the Schrödinger equation and analyzes the regularity of ψ in the random space. In Section 3, we introduce the Gaussian wave packet transform and prove that the w equation is not oscillatory in the random space. Section 5 shows extensive numerical tests by using the stochastic collocation method to demonstrate the efficiency and accuracy of our proposed scheme. Relations of different numbers of the collocation points needed in each step of the implementation will be explained and studied numerically. Conclusion and future work are given in Section 6.

2 The semi-classical Schrödinger equation with random inputs

2.1 The semi-classical limit with random inputs

In this part, we investigate the semi-classical limit of the Schrödinger equation with random inputs by the Wigner transform [6, 10, 1, 17]. Obviously, the potential function $V(\mathbf{x}, \mathbf{z})$ can be decomposed as

$$V(\mathbf{x}, \mathbf{z}) = \bar{V}(\mathbf{x}) + N(\mathbf{x}, \mathbf{z}), \tag{2.4}$$

such that

$$\langle V \rangle_\pi = \bar{V}, \quad \langle N \rangle_\pi = 0.$$

For $f, g \in L^2(\mathbb{R}^d)$, the Wigner transform is defined as a phase-space function

$$W^\varepsilon(f, g)(t, \mathbf{x}, \boldsymbol{\xi}) = \frac{1}{(2\pi)^d} \int_{\mathbb{R}^d} e^{i\mathbf{y}\cdot\boldsymbol{\xi}} \bar{f}\left(\mathbf{x} + \frac{\varepsilon}{2}\mathbf{y}\right) g\left(\mathbf{x} - \frac{\varepsilon}{2}\mathbf{y}\right) d\mathbf{y}. \tag{2.5}$$

Recall that $\psi^\varepsilon(t, \mathbf{x})$ is the exact solution of equation (1.1). Denote $W^\varepsilon(t, \mathbf{x}, \boldsymbol{\xi}, \mathbf{z}) = W^\varepsilon(\psi^\varepsilon, \psi^\varepsilon)$, it is possible to prove that W^ε satisfies the Wigner equation [6, 2]

$$\partial_t W^\varepsilon + \boldsymbol{\xi} \cdot \nabla_\mathbf{x} W^\varepsilon + \Theta[V]W^\varepsilon = 0, \tag{2.6}$$

in which $\Theta[V]W^\varepsilon$ is a pseudo-differential operator acting on W^ε defined by

$$\Theta[V]W^\varepsilon := \frac{i}{(2\pi)^d \varepsilon} \int_{\mathbb{R}^d} \left(V\left(\mathbf{x} + \frac{\varepsilon}{2}\boldsymbol{\alpha}\right) - V\left(\mathbf{x} - \frac{\varepsilon}{2}\boldsymbol{\alpha}\right)\right) \hat{W}^\varepsilon(t, \mathbf{x}, \boldsymbol{\alpha}, \mathbf{z}) e^{i\boldsymbol{\alpha}\cdot\boldsymbol{\xi}} d\boldsymbol{\alpha}. \tag{2.7}$$

By Weyl's Calculus (see [6]) as $\varepsilon \to 0$, the Wigner measure $W^0 = \lim_{\varepsilon\to 0} W^\varepsilon(u^\varepsilon, u^\varepsilon)$ satisfies the classical Liouville equation

$$W_t^0 + \boldsymbol{\xi} \cdot \nabla_\mathbf{x} W^0 - \nabla_\mathbf{x} V \cdot \nabla_{\boldsymbol{\xi}} W^0 = 0, \tag{2.8}$$

4

with

$$W^0(t = 0, \mathbf{x}, \boldsymbol{\xi}, \mathbf{z}) = W_I^0(\mathbf{x}, \boldsymbol{\xi}, \mathbf{z}) := \lim_{\varepsilon \to 0} W^\varepsilon(\psi_0^\varepsilon, \psi_0^\varepsilon). \tag{2.9}$$

All the limits above are defined in an appropriate weak sense (see [6, 17]).

With the decomposition of the potential as in (2.4), the classical Liouville equation becomes

$$W_t^0 + \boldsymbol{\xi} \cdot \nabla_\mathbf{x} W^0 - \nabla_\mathbf{x} \bar{V} \cdot \nabla_{\boldsymbol{\xi}} W^0 - \nabla_\mathbf{x} N \cdot \nabla_{\boldsymbol{\xi}} W^0 = 0. \tag{2.10}$$

This clearly shows, due to the random potential, the bi-characteristics of the Liouville equation contains the random force term with $\langle -\nabla_\mathbf{x} N \rangle_\pi = -\nabla_\mathbf{x} \langle N \rangle_\pi = 0$, and the characteristic equations are

$$\begin{cases} \dot{\mathbf{x}} = \boldsymbol{\xi}, \\ \dot{\boldsymbol{\xi}} = -\nabla_\mathbf{x} \bar{V} - \nabla_\mathbf{x} N. \end{cases} \tag{2.11}$$

Also, by definition, it is easy to check that $\forall \mathbf{z} \in I_\mathbf{z}$, W^ε is real-valued. To sum up, in the semi-classical limit, the Wigner measure W^0 picks up the dependence of the random variable $\mathbf{z}$ though the initial condition and the vector field $\nabla_\mathbf{x} N$.

Next, we discuss if one can derive the averaged equation to integrate out the random variable $\mathbf{z}$. In equation (2.10), by taking the average with respect to the random variable $\mathbf{z}$, one gets

$$\partial_t \langle W^0 \rangle_\pi + \boldsymbol{\xi} \cdot \nabla_\mathbf{x} \langle W^0 \rangle_\pi - \nabla_\mathbf{x} \bar{V} \cdot \nabla_{\boldsymbol{\xi}} \langle W^0 \rangle_\pi - \langle \nabla_\mathbf{x} N \cdot \nabla_{\boldsymbol{\xi}} W^0 \rangle_\pi.$$

Notice that, in the last term, both N and W^0 depend on $\mathbf{z}$, thus it cannot be directly written as a term involving $\langle W^0 \rangle_\pi$, rather it connects with the covariance of $\nabla_\mathbf{x} N$ and $\nabla_{\boldsymbol{\xi}} W^0$. In fact,

$$\begin{aligned} -\langle \nabla_\mathbf{x} N \cdot \nabla_{\boldsymbol{\xi}} W^0 \rangle_\pi &= -\langle (\nabla_\mathbf{x} N - \nabla_\mathbf{x} \langle N \rangle_\pi) \cdot (\nabla_{\boldsymbol{\xi}} W^0 - \nabla_{\boldsymbol{\xi}} \langle W^0 \rangle_\pi) \rangle_\pi - \nabla_\mathbf{x} \langle N \rangle_\pi \cdot \nabla_{\boldsymbol{\xi}} \langle W^0 \rangle_\pi \\ &= -\text{Cov}(\nabla_\mathbf{x} N, \nabla_{\boldsymbol{\xi}} W^0), \end{aligned}$$

since $\nabla_\mathbf{x} \langle N \rangle_\pi = 0$.

To illustrate the effect of the random potential, we consider the following special case

$$\bar{V} = \frac{1}{2} |\mathbf{x}|^2, \quad N = -\mathbf{x} \cdot \mathbf{g}(\mathbf{z}).$$

In this case, the Liouville equation simplifies to

$$W_t^0 + \boldsymbol{\xi} \cdot \nabla_\mathbf{x} W^0 - \mathbf{x} \cdot \nabla_{\boldsymbol{\xi}} W^0 + \mathbf{g}(\mathbf{z}) \cdot \nabla_{\boldsymbol{\xi}} W^0 = 0. \tag{2.12}$$

Then, if one considers the following change of variables

$$\mathbf{x} = \tilde{\mathbf{x}} + \mathbf{g}(\mathbf{z}), \quad \boldsymbol{\xi} = \tilde{\boldsymbol{\xi}},$$

then, equation (2.12) becomes

$$W_t^0 + \tilde{\boldsymbol{\xi}} \cdot \nabla_{\tilde{\mathbf{x}}} W^0 - \tilde{\mathbf{x}} \cdot \nabla_{\tilde{\boldsymbol{\xi}}} W^0 = 0. \tag{2.13}$$

5

And correspondingly, the initial condition becomes

$$W^0(t = 0, \tilde{\mathbf{x}}, \tilde{\boldsymbol{\xi}}, \mathbf{z}) = W_I^0(\tilde{\mathbf{x}} + \mathbf{g}(\mathbf{z}), \tilde{\boldsymbol{\xi}}).$$

Thus, the average with respect to the random variable $\mathbf{z}$ can be taken and one gets a closed equation for $\langle W^0 \rangle_\pi$,

$$\partial_t \langle W^0 \rangle_\pi + \tilde{\boldsymbol{\xi}} \cdot \nabla_{\tilde{\mathbf{x}}} \langle W^0 \rangle_\pi - \tilde{\mathbf{x}} \cdot \nabla_{\tilde{\boldsymbol{\xi}}} \langle W^0 \rangle_\pi = 0. \tag{2.14}$$

and

$$\langle W^0 \rangle_\pi (t = 0, \tilde{\mathbf{x}}, \tilde{\boldsymbol{\xi}}) = \langle W_I^0(\tilde{\mathbf{x}} + \mathbf{g}(\cdot), \tilde{\boldsymbol{\xi}}) \rangle_\pi.$$

This example shows that the randomness in the slow-varying potential changes the transport part of the Liouville equation, although in the averaged equation the transport structure may be even unchanged.

When the potential is random and with a general form of z dependence, the two processes of a) first pushing $\varepsilon \to 0$ then taking expected value in z of the classical limit (the Liouville equation); and b) first taking expected value in z on the Wigner equation then letting $\varepsilon \to 0$ do not commute. Though numerically, our simulation results seem to suggest the commutation of these two iterated processes. In later section we will make a numerical comparison to show that the expected values of the position density and flux do converge in the $\varepsilon \to 0$ limit.

To conclude this part, we remark that in [1, 23] and subsequent works, the authors have considered apparently a related but fundamentally different model, where the unperturbed system is the semi-classical Schrödinger with fast-varying smaller magnitude and random perturbation in the potential is also fast-varying. And they show that the randomness in that scaling introduces additional scattering terms in the limit equations, while in our case the randomness only persist in the initial data and the force field in the limit equation.

2.2 Regularity of ψ in the z variable

The semi-classical Schrödinger equation is a family of dispersive wave equations parameterized by $\varepsilon \ll 1$, and it is well known that the wave equation propagates $O(\varepsilon)$ scaled oscillations in space and time. However, it is not clear yet whether the small parameter ε induces oscillations in the random variable $\mathbf{z}$.

Here and in subsection 3.2, we will conduct a regularity analysis of ψ in the random space, which enables us to study the oscillatory behavior of solutions in the random space, which gives guidance on how many collocation points needed in each step of the collocation method should depend on the scaled constant ε.

To investigate the regularity of the wave function in the $\mathbf{z}$ variable, we check the following averaged norm

$$||f||_\Gamma := \left(\int_{I_z} \int_{\mathbb{R}^3} |f(t, \mathbf{x}, \mathbf{z})|^2 \; d\mathbf{x} \pi(\mathbf{z}) d\mathbf{z} \right)^{\frac{1}{2}}. \tag{2.15}$$

To be more precise, (2.15) denotes the square root of the expected value in $\mathbf{z}$ of the square of the $L^2(x)$ norm of f. We name it Γ-norm for short.

One first observes that $\forall\, \mathbf{z} \in I_{\mathbf{z}}$,

$$\frac{\partial}{\partial t}\|\psi^\varepsilon\|_{L_{\mathbf{x}}^2}^2(t, \mathbf{z}) = 0,$$

thus

$$\frac{d}{dt}\|\psi^\varepsilon\|_\Gamma^2 = 0,$$

which means the Γ-norm of the wave function ψ^ε is conserved in time,

$$\|\psi^\varepsilon\|_\Gamma(t) = \|\psi_{\mathrm{in}}^\varepsilon\|_\Gamma.$$

However, we show in the following that ψ^ε has ε-scaled oscillations in $\mathbf{z}$ even if V and $\psi_{\mathrm{in}}^\varepsilon$ do not have ε-dependent oscillations in $\mathbf{z}$. We first examine the first-order partial derivative of ψ^ε in z_1, and denote $\psi^1 = \psi_{z_1}^\varepsilon$ and $V^1 = V_{z_1}$, then by differentiating the semi-classical schrödinger equation (1.1) with respect to z_1, one gets

$$i\varepsilon\psi_t^1 = -\frac{\varepsilon^2}{2}\Delta_{\mathbf{x}}\psi^1 + V^1\psi^\varepsilon + V\psi^1.$$

By direct calculation,

$$\begin{aligned}
\frac{d}{dt}\|\psi^1\|_\Gamma^2 &= \int \left(\psi_t^1\bar{\psi}^1 + \psi^1\bar{\psi}_t^1\right)\pi d\mathbf{x}d\mathbf{z} \\
&= \int \left(\frac{1}{i\varepsilon}V^1\psi^\varepsilon\bar{\psi}^1 - \frac{1}{i\varepsilon}V^1\psi^1\bar{\psi}^\varepsilon\right)\pi d\mathbf{x}d\mathbf{z} \\
&\leqslant \frac{2}{\varepsilon}\|\psi^1\|_\Gamma\,\|V^1\psi^\varepsilon\|_\Gamma,
\end{aligned}$$

where the Cauchy-Schwarz inequality and the Jensen inequality are used in the last step, more specifically,

$$\int V^1\psi^\varepsilon\bar{\psi}^1 dx \leq \left(\int (V^1\psi^\varepsilon)^2 dx\right)^{1/2}\left(\int (\bar{\psi}^1)^2 dx\right)^{1/2},$$

$$\int\int V^1\psi^\varepsilon\bar{\psi}^1 dx\,\pi(z)dz \leq \left(\int \left(\int V^1\psi^\varepsilon\bar{\psi}^1 dx\right)^2 \pi(z)dz\right)^{1/2} \leq \|V^1\psi^\varepsilon\|_\Gamma\,\|\psi^1\|_\Gamma.$$

Thus

$$\frac{d}{dt}\|\psi^1\|_\Gamma \leqslant \frac{1}{\varepsilon}\|V^1\psi^\varepsilon\|_\Gamma^2,$$

For $t = O(1)$, the pessimistic estimate implies

$$\|\psi^1\|_\Gamma = O(\varepsilon^{-1}).$$

Moreover, for $\mathbf{k} = (k_1, k_2, \cdots, k_n) \in \mathbb{N}^n$, denote $|\mathbf{k}| = \sum_{j=1}^n k_j$, we can similarly conclude that

$$\|\partial_{\mathbf{z}}^{\mathbf{k}}\psi^\varepsilon\|_\Gamma = O(\varepsilon^{-|\mathbf{k}|}). \tag{2.16}$$

7

Although the estimates above are apparently pessimistic, we would like to show that the high frequency oscillations in $\mathbf{z}$ can be seen in the following example. For simplicity, we consider x be one dimensional. If the potential V is quadratic in x, it has been shown by Heller in [9] that,

$$\phi(x,t) = \exp\left[i\frac{\alpha(t)\big(x-q(t)\big)^2 - p(t)\big(x-q(t)\big) + \gamma(t)}{\varepsilon}\right] \qquad (2.17)$$

is an exact solution to the semi-classical Schrödinger equation, provided that, $q(t)$, $p(t)$, $\alpha(t)$ and $\gamma(t)$ satisfy the following system of equations

$$\begin{cases} \dot{q} = p, \\ \dot{p} = -V_q(q), \\ \dot{\alpha} = -2\alpha^2 - \frac{1}{2}V_{qq}(q), \\ \dot{\gamma} = \frac{1}{2}p^2 - V(q) + i\varepsilon\alpha. \end{cases} \qquad (2.18)$$

Due to the same reason,

$$\Phi(t,x,\mathbf{z}) = \exp\left[i\frac{\alpha(t,\mathbf{z})\big(x-q(t,\mathbf{z})\big)^2 - p(t,\mathbf{z})\big(x-q(t,\mathbf{z})\big) + \gamma(t,\mathbf{z})}{\varepsilon}\right]$$

is an exact solution to equation (1.1), when potential $V(x,\mathbf{z})$ is quadratic in x. Clearly, this specific solution saturates the estimate (2.16), which implies, even if initially ψ^ε is smooth in $\mathbf{z}$, it will pick up ε-dependent oscillations in the $\mathbf{z}$ variables. In Section 5, we will also show numerically the ε-scaled oscillations of such wave functions in the $\mathbf{z}$ variable.

To conclude this section, we emphasize the numerical challenges with respect to the random variable $\mathbf{z}$. Due to the oscillatory behavior in $\mathbf{z}$, if one applies the generalized polynomial chaos (gPC)-based stochastic methods directly to the semi-classical Schrödinger equation, one needs at least ε-dependent basis functions or quadrature points to get an accurate approximation. The stochastic collocation method will be discussed in detail in subsection 5.1.

3 The semi-classical Schrödinger equation and the Gaussian wave packet transformation

To overcome the numerical burdens in sampling the random variable z, we introduce the Gaussian wave packet transformation (abbreviated by GWPT), which has been proven to be a very efficient tool for computing the Schrödinger equation in the high frequency regime. In essence, the GWPT equivalently transforms the highly oscillatory wave equation to w, thus facilitate the design of efficient numerical methods. The main goal of this section is to study the *uniform regularity* of w in the $\mathbf{z}$ variable, and conclude that the number of basis functions or quadrature points is *independent of ε*, if applying the SG or SC method in our GWPT framework.

3.1 Review of the Gaussian wave packet transformation

First, we briefly summarize the Gaussian wave packet transformation applied to the semi-classical Schrödinger equation with random inputs, which is a natural extension of the GWPT method for the deterministic problem [26]. Consider the semi-classical Schrödinger equation given by (1.1)–(1.2). Note that in this work, random inputs are assumed to be classical, thus we only consider the cases when the wave packet position and momentum in the GWPT parameters depend on the random variable $\mathbf{z}$.

We start by the following *ansatz*

$$\psi(t, \mathbf{x}, \mathbf{z}) = \widetilde{w}(t, \boldsymbol{\xi}, \mathbf{z}) \exp\left(g(t, \boldsymbol{\xi}, \mathbf{z})\right) := \widetilde{w}(t, \boldsymbol{\xi}, \mathbf{z}) \exp\left(i\left(\boldsymbol{\xi}^T \boldsymbol{\alpha}_R \boldsymbol{\xi} + \mathbf{p}^T \boldsymbol{\xi} + \gamma\right)/\varepsilon\right), \quad (3.19)$$

where $\boldsymbol{\xi} = \mathbf{x} - \mathbf{q}$, $\boldsymbol{\alpha}_R$ is a real-valued symmetric matrix and γ is a complex-valued scalar.

Denote $\boldsymbol{\alpha}_R = \mathrm{Re}(\boldsymbol{\alpha})$, $\boldsymbol{\alpha}_I = \mathrm{Im}(\boldsymbol{\alpha})$ and $\boldsymbol{\alpha} = \boldsymbol{\alpha}_R + i\boldsymbol{\alpha}_I$. Insert the ansatz (3.19) into (1.1), then $\widetilde{w}(t, \boldsymbol{\xi}, \mathbf{z})$ satisfies

$$\widetilde{w}_t = -2\,\boldsymbol{\xi}^T \boldsymbol{\alpha}_R \nabla_{\boldsymbol{\xi}} \widetilde{w} + \frac{i\varepsilon}{2} \Delta_{\boldsymbol{\xi}} \widetilde{w} - \frac{i}{\varepsilon}\left(U_r + 2\,\boldsymbol{\xi}^T \boldsymbol{\alpha}_I^2\,\boldsymbol{\xi}\right)\widetilde{w},$$

provided $\mathbf{p}$, $\mathbf{q}$, $\boldsymbol{\alpha}$ satisfy the following equations

$$\begin{cases} \dot{\mathbf{q}} = \mathbf{p}, \\ \dot{\mathbf{p}} = -\nabla V(\mathbf{q}), \\ \dot{\boldsymbol{\alpha}} = -2\,\boldsymbol{\alpha}^2 - \frac{1}{2}\nabla\nabla V(\mathbf{q}), \\ \dot{\gamma} = \frac{1}{2}\mathbf{p}^T\mathbf{p} - V(\mathbf{q}) + i\varepsilon\,\mathrm{Tr}(\boldsymbol{\alpha}_R), \end{cases} \quad (3.20)$$

while

$$U_r = V(\boldsymbol{\xi} + \mathbf{q}) - V(\mathbf{q}) - \boldsymbol{\xi}^T \nabla V(\mathbf{q}) - \frac{1}{2}\boldsymbol{\xi}^T \nabla^2 V(\mathbf{q})\boldsymbol{\xi}.$$

At last, introduce the change of variables $\widetilde{w}(t, \boldsymbol{\xi}, \mathbf{z}) = w(t, \boldsymbol{\eta}, \mathbf{z})$, where

$$\boldsymbol{\eta} = \mathbf{B}\boldsymbol{\xi}/\sqrt{\varepsilon}, \quad (3.21)$$

with

$$\dot{\mathbf{B}} = -2\mathbf{B}\,\boldsymbol{\alpha}_R, \qquad \mathbf{B}(0) = \sqrt{\boldsymbol{\alpha}_I(0)},$$

then $\boldsymbol{\alpha}_I = \mathbf{B}^T\mathbf{B}$ and

$$w_t = \frac{i}{2}\,\mathrm{Tr}\left(\mathbf{B}^T \nabla_{\boldsymbol{\eta}}^2 w\,\mathbf{B}\right) - 2i\,\boldsymbol{\eta}^T (\mathbf{B}^T)^{-1}\boldsymbol{\alpha}_I^2\,\mathbf{B}^{-1}\boldsymbol{\eta}w + \frac{1}{i\varepsilon}U_r w, \quad (3.22)$$

Note that in the $\boldsymbol{\eta}$ variable,

$$\frac{1}{i\varepsilon}U_r = O(\sqrt{\varepsilon}),$$

so the w equation (3.22) is not oscillatory in $\boldsymbol{\eta}$ nor in t. Furthermore, if one drops those $O(\sqrt{\varepsilon})$ terms, one expects to recover the leading order Gaussian beam method [27].

In our numerical tests, we will only consider the initial data ψ given by a Gaussian wave packet, i.e.

$$\psi(0, \mathbf{x}, \mathbf{z}) = \exp\left(i\left(\boldsymbol{\xi}^T \boldsymbol{\alpha}\,\boldsymbol{\xi} + \mathbf{p}^T \boldsymbol{\xi} + \gamma\right)/\varepsilon\right), \quad (3.23)$$

More general initial conditions, (with a numerical support proportional to $\sqrt{\varepsilon}$) can be approximated with the desired accuracy as a superposition of relatively small number of Gaussian wave packets. See [26, Section 2.6] for more details.

9

3.2 Regularity of w in the z variable

It is well understood that the w equation no longer propagates ε-dependent oscillations in space or in time. We show in the following that the w equation is not oscillatory in the **z** variable either. In this section, we assume the spatial variable x, η is one dimensional to simplify the analysis. Now the w equation (3.22) reduces to

$$w_t = \frac{i}{2}\alpha_I w_{\eta\eta} - 2i\alpha_I \eta^2 w + \frac{U_r}{i\varepsilon}w, \tag{3.24}$$

where

$$U_r(t,\eta,\mathbf{z}) = V(q + \sqrt{\varepsilon}B^{-1}\eta, \mathbf{z}) - V(q,\mathbf{z}) - \sqrt{\varepsilon}B^{-1}\eta\, V_x(q,\mathbf{z}) - \frac{1}{2}\left(\sqrt{\varepsilon}B^{-1}\eta\right)^2 V_{xx}(q,\mathbf{z}),$$

and $B = \sqrt{\alpha_I}$. Observe that $w = w(t,\eta;\mathbf{z})$ is a function of independent variables (t,η), but it obtains the dependence of the parameter **z** through the coefficients. We emphasize that, although the change of variable (3.21) is **z** dependent, in the w equation, η and **z** are independent variables. This is due to the fact that it is $w = w(t,\eta;\mathbf{z})$, not $w = w(t,\eta(\mathbf{z});\mathbf{z})$. With the random inputs, the Gaussian wave packet transform is straightforward for all **z**. Besides the time dependence, the Gaussian wave packet parameters q, p, α, B and γ also depend on **z**. The smooth components w and U_r depend on **z**. Then, it is not yet clear whether w has ε dependent z derivatives.

We make the assumption that the potential is infinitely smooth with bounded derivatives in both x and **z**, namely, for $m \in \mathbb{N}$ and $\mathbf{k} = (k_1, k_2, \cdots, k_n) \in \mathbb{N}^n$, there exists a constant $C_{m,\mathbf{k}}$ such that,

$$|\partial_x^m \partial_{\mathbf{z}}^{\mathbf{k}} V| \leqslant C_{m,\mathbf{k}}, \tag{3.25}$$

where $\partial_{\mathbf{z}}^{\mathbf{k}} = \partial_{z_1}^{k_1} \cdots \partial_{z_n}^{k_n}$. We also assume that the w equation (3.24) is equipped with an initial condition, $w(0,\eta,\mathbf{z}) = w_{\text{in}}(\eta,\mathbf{z})$, which has a $O(1)$ sized support, satisfying the following assumption: for $m \in \mathbb{N}$ and $\mathbf{k} = (k_1, k_2, \cdots, k_n) \in \mathbb{N}^n$, there exists an ε-independent constant $C_{m,\mathbf{k}}$ such that,

$$\|\partial_\eta^m \partial_{\mathbf{z}}^{\mathbf{k}} w_{\text{in}}\|_\Gamma \leqslant C_{m,\mathbf{k}}. \tag{3.26}$$

Our goal is to show that the smoothness in the **z** variable will be preserved in time. Before calculating the regularity of w in the **z** variable, we first show Lemma 3.1 and Lemma 3.2, which will be used for the main result of this section namely Theorem 3.1.

LEMMA 3.1. *Assume boundedness condition (3.25), and initial data for wave packet parameters satisfying the following: there exists an ε independent constant $C_{\mathbf{K}}$, such that*

$$|\partial_{\mathbf{z}}^{\mathbf{k}} q(0)| \leqslant C_{\mathbf{K}}, \quad |\partial_{\mathbf{z}}^{\mathbf{k}} p(0)| \leqslant C_{\mathbf{K}}, \quad |\partial_{\mathbf{z}}^{\mathbf{k}} \alpha(0)| \leqslant C_{\mathbf{K}}.$$

Then, there exists an ε independent constant $C_{T,\mathbf{K}}$, such that for $t \in [0,T]$,

$$|\partial_{\mathbf{z}}^{\mathbf{k}} q(t)| \leqslant C_{T,\mathbf{K}}, \quad |\partial_{\mathbf{z}}^{\mathbf{k}} p(t)| \leqslant C_{T,\mathbf{K}}, \quad |\partial_{\mathbf{z}}^{\mathbf{k}} \alpha(t)| \leqslant C_{T,\mathbf{K}}.$$

The proof follows standard estimations of the ODE system of the parameters, which we shall omit here. We also remark that we have only listed the parameters needed for showing the regularity properties of the w equation (3.24), but this argument clearly works for other wave packets parameters as well.

LEMMA 3.2. *With the boundedness assumptions (3.25), for all* $\mathbf{k} = (k_1, k_2, \cdots, k_n) \in \mathbb{N}^n$, *it is*

$$\partial_{\mathbf{z}}^{\mathbf{k}} U_r = O(\varepsilon^{\frac{3}{2}}).$$

Proof. Recall that

$$U_r(t, \eta, \mathbf{z}) = V(q + \sqrt{\varepsilon} B^{-1} \eta, \mathbf{z}) - V(q, \mathbf{z}) - \sqrt{\varepsilon} B^{-1} \eta \, V_x(q, \mathbf{z}) - \frac{1}{2} \left(\sqrt{\varepsilon} B^{-1} \eta \right)^2 V_{xx}(q, \mathbf{z}). \quad (3.27)$$

We observe that, assumption (3.25) together with the Taylor's Theorem implies, for $m \in \mathbb{N}$ and $\mathbf{k} = (k_1, k_2, \cdots, k_n) \in \mathbb{N}^n$,

$$T_{m,\mathbf{k}} := \partial_x^m \partial_{\mathbf{z}}^{\mathbf{k}} V(q + \sqrt{\varepsilon} B^{-1} \eta, \mathbf{z}) - \partial_x^m \partial_{\mathbf{z}}^{\mathbf{k}} V(q, \mathbf{z}) - \sqrt{\varepsilon} B^{-1} \eta \partial_x^{m+1} \partial_{\mathbf{z}}^{\mathbf{k}} V(q, \mathbf{z})$$
$$- \frac{1}{2} \left(\sqrt{\varepsilon} B^{-1} \eta \right)^2 \partial_x^{m+2} \partial_{\mathbf{z}}^{\mathbf{k}} V(q, \mathbf{z}) = O(\varepsilon^{\frac{3}{2}}). \quad (3.28)$$

Thus, it is clear that $|U_r| = O(\varepsilon^{\frac{3}{2}})$.

Next, we examine the first order derivative in z_1. By direct calculation,

$$\partial_{z_1} U_r = \partial_{z_1} V(q + \sqrt{\varepsilon} B^{-1} \eta, \mathbf{z}) + \partial_x V(q + \sqrt{\varepsilon} B^{-1} \eta, \mathbf{z}) \partial_{z_1} (q + \sqrt{\varepsilon} B^{-1} \eta)$$
$$- \left(\partial_{z_1} V(q, z) + \partial_x V(q, \mathbf{z}) \partial_{z_1} q \right)$$
$$- \left(\partial_{z_1} (\sqrt{\varepsilon} B^{-1} \eta) \partial_x V(q, \mathbf{z}) + \sqrt{\varepsilon} B^{-1} \eta \, \partial_{xz_1} V(q, \mathbf{z}) + \sqrt{\varepsilon} B^{-1} \eta \, \partial_{xx} V(q, \mathbf{z}) \partial_{z_1} q \right)$$
$$- \frac{1}{2} \varepsilon \left(\partial_{z_1} (B^{-1} \eta)^2 \partial_{xx} V(q, \mathbf{z}) + (B^{-1} \eta)^2 \partial_{xxz_1} V(q, \mathbf{z}) + (B^{-1} \eta)^2 \partial_{xxx} V(q, \mathbf{z}) \partial_{z_1} q \right)$$
$$= \partial_{z_1} V(q + \sqrt{\varepsilon} B^{-1} \eta, \mathbf{z}) - \partial_{z_1} V(q, z)$$
$$- \sqrt{\varepsilon} B^{-1} \eta \, \partial_{xz_1} V(q, \mathbf{z}) - \frac{1}{2} (B^{-1} \eta)^2 \partial_{xxz_1} V(q, \mathbf{z})$$
$$+ \partial_x V(q + \sqrt{\varepsilon} B^{-1} \eta, \mathbf{z}) \partial_{z_1} q - \partial_x V(q, \mathbf{z}) \partial_{z_1} q$$
$$- \sqrt{\varepsilon} B^{-1} \eta \, \partial_{xx} V(q, \mathbf{z}) \partial_{z_1} q - \frac{1}{2} (B^{-1} \eta)^2 \partial_{xxx} V(q, \mathbf{z}) \partial_{z_1} q$$
$$+ \left(\partial_x V(q + \sqrt{\varepsilon} B^{-1} \eta, \mathbf{z}) - \partial_x V(q, \mathbf{z}) - \sqrt{\varepsilon} B^{-1} \eta \, \partial_{xx} V(q, \mathbf{z}) \right) \partial_{z_1} (\sqrt{\varepsilon} B^{-1} \eta).$$

Thus, by (3.28) and Lemma 3.1, we conclude that $\partial_{z_1} U_r = O(\varepsilon^{\frac{3}{2}})$.

By induction, one easily sees that $\partial_{\mathbf{z}}^{\mathbf{k}} U_r$ is a summation of products of $T_{m,\mathbf{k}}$ (add up with some other terms). Hence, by (3.28) and Lemma 3.1, it can be concluded that $\partial_{\mathbf{z}}^{\mathbf{k}} U_r = O(\varepsilon^{\frac{3}{2}})$, and the lemma follows. $\qquad \square$

We give the definition of the averaged norm of $w = w(t, \eta, \mathbf{z})$,

$$||w||_{\mathcal{T}}^2 := \langle ||w||_{L^2(\eta)}^2 \rangle_{\pi(\mathbf{z})},$$

which is analogous to the Γ–norm defined in (2.15) for ψ while using η variable in the $L^2(\eta)$ norm here. We now present the main theorem of this section:

11

THEOREM 3.1. *With the boundedness assumptions* (3.25) *and conditions on the initial data* (3.26), *the w equation* (3.24) *preserves the regularity in the following sense: for a fixed $T > 0$, $\mathbf{k} = (k_1, k_2, \cdots, k_n) \in \mathbb{N}^n$, there exists an ε-independent constant $M_{T,\mathbf{k}}$, such that for $0 \leqslant t \leqslant T$,*

$$||\partial_{\mathbf{z}}^{\mathbf{k}} w||_{\mathcal{T}} \leqslant M_{T,\mathbf{k}} \,. \tag{3.29}$$

Proof. The w equation can be written as

$$w_t = \frac{i}{2}\alpha_I w_{\eta\eta} - i\tilde{U}w, \tag{3.30}$$

where

$$\tilde{U} = 2\alpha_I \eta^2 + \frac{U_r}{\varepsilon},$$

and U_r given in (3.27). We first look at the $\mathcal{T}$-norm of w,

$$\frac{d}{dt}||w||_{\mathcal{T}}^2 = \int (w\bar{w})_t \, d\eta\pi(\mathbf{z})d\mathbf{z} = \int (w_t\bar{w} + w\bar{w}_t) \, d\eta\pi(\mathbf{z})d\mathbf{z}$$

$$= \int \big(\frac{i}{2}\alpha_I w_{\eta\eta} - i\tilde{U}w\big)\bar{w} + w\big(-\frac{i}{2}\alpha_I \bar{w}_{\eta\eta} + i\tilde{U}\bar{w}\big)\big) \, d\eta\pi(\mathbf{z})d\mathbf{z} = 0,$$

which implies the averaged norm of w is preserved, $||w||_{\mathcal{T}} = ||w_{\text{in}}||_{\mathcal{T}}$.

Differentiating (3.30) with respect to z_1, by the chain rule, one has

$$\partial_t \partial_{z_1} w = \frac{i}{2}\big(\partial_{z_1}\alpha_I \, w_{\eta\eta} + \alpha_I w_{\eta\eta z_1}\big) - i\partial_{z_1}\tilde{U}w - i\tilde{U}\partial_{z_1}w.$$

By direct calculation (omit the $\mathcal{T}$-subscript in the norm $||\cdot||_{\mathcal{T}}$ for notation simplicity),

$$\frac{d}{dt}||\partial_{z_1}w||^2 = \int (\partial_t\partial_{z_1}w \, \partial_{z_1}\bar{w} + \partial_{z_1}w \, \partial_t\partial_{z_1}\bar{w}) \, d\eta\pi(\mathbf{z})d\mathbf{z}$$

$$= \int \bigg(\Big[\frac{i}{2}\big(\partial_{z_1}\alpha_I \, w_{\eta\eta} + \alpha_I w_{\eta\eta z_1}\big) - i\partial_{z_1}\tilde{U}w - i\tilde{U}\partial_{z_1}w\Big]\partial_{z_1}\bar{w}$$

$$+ \partial_{z_1}w\Big[-\frac{i}{2}\big(\partial_{z_1}\alpha_I \, \bar{w}_{\eta\eta} + \alpha_I \bar{w}_{\eta\eta z_1}\big) + i\partial_{z_1}\tilde{U}\bar{w} + i\tilde{U}\partial_{z_1}\bar{w}\big)\Big]\bigg) \, d\eta\pi(\mathbf{z})d\mathbf{z}$$

$$= \int \Big[\frac{i}{2}\partial_{z_1}\alpha_I(w_{\eta\eta} \, \partial_{z_1}\bar{w} - \partial_{z_1}w \, \bar{w}_{\eta\eta}) + i\partial_{z_1}\tilde{U}(-w \, \partial_{z_1}\bar{w} + \partial_{z_1}w \, \bar{w})\Big] \, d\eta\pi(\mathbf{z})d\mathbf{z}$$

$$\leq ||\partial_{z_1}w|| \, ||\partial_{z_1}\alpha_I \, w_{\eta\eta}|| + 2||\partial_{z_1}\tilde{U}w|| \, ||\partial_{z_1}w||,$$

where integration by parts and the Cauchy-Schwarz inequality are used. Thus

$$\frac{d}{dt}||\partial_{z_1}w|| \leq \frac{1}{2}||\partial_{z_1}\alpha_I \, w_{\eta\eta}|| + ||\partial_{z_1}\tilde{U}w||. \tag{3.31}$$

Clearly, to prove the boundedness of $||\partial_{z_1}w||$, it suffices to show the boundedness of the right hand side of (3.31). Fortunately, the right hand side of (3.31) does not involve the $\mathbf{z}$ derivative of w. The estimates of the η derivatives of w are standard, which can be carried out in the following deductive way.

12

We calculate that

$$
\begin{aligned}
\frac{d}{dt}||w_\eta||^2 &= \int \big((w_t)_\eta \bar{w}_\eta + w_\eta (\bar{w}_t)_\eta\big) d\eta \pi(\mathbf{z}) d\mathbf{z} \\
&= \int \big(-i(\tilde{U}w)_\eta \bar{w}_\eta + i w_\eta (\tilde{U}\bar{w})_\eta\big) d\eta \pi(\mathbf{z}) d\mathbf{z} \\
&\leqslant \left(\int (\tilde{U}w)_\eta^2 \bar{w}_\eta^2 \, d\eta \pi(\mathbf{z}) d\mathbf{z}\right)^{1/2} \left((\tilde{U}\bar{w})_\eta^2 \, w_\eta^2 \, d\eta \pi(\mathbf{z}) d\mathbf{z}\right)^{1/2} \\
&= 2||w_\eta|| \, ||(\tilde{U}w)_\eta||.
\end{aligned}
\tag{3.32}
$$

Since $\partial_\eta \tilde{U} = 4\alpha_I \eta + \partial_\eta U_r/\varepsilon = O(1)$, and by the chain rule,

$$
||(\tilde{U}w)_\eta|| = ||\tilde{U}_\eta w + \tilde{U}w_\eta|| \leq C_1||w|| + C_2||w_\eta||,
$$

where $C_1, C_2 > 0$ are constants. Thus

$$
\frac{d}{dt}||w_\eta|| \leq C_1||w|| + C_2||w_\eta||.
\tag{3.33}
$$

For $t \in [0,T]$, the boundedness of $||w_\eta||$ follows from the Grönwall's inequality and assumption (3.26). Similarly, we get

$$
\begin{aligned}
\frac{d}{dt}||w_{\eta\eta}||^2 &= \int \big((w_t)_{\eta\eta} \bar{w}_{\eta\eta} + w_{\eta\eta} (\bar{w}_t)_{\eta\eta}\big) d\eta \pi(\mathbf{z}) d\mathbf{z} \\
&= \int \big(-i(\tilde{U}w)_{\eta\eta} \bar{w}_{\eta\eta} + i w_{\eta\eta} (\tilde{U}\bar{w})_{\eta\eta}\big) d\eta \pi(\mathbf{z}) d\mathbf{z} \\
&\leqslant 2||w_{\eta\eta}|| \, ||(\tilde{U}w)_{\eta\eta}||,
\end{aligned}
$$

where the Cauchy-Schwarz inequality is used again just as in (3.32). By the chain rule, $\exists\, C_1, C_2, C_3 \in \mathbb{R}$ such that

$$
||(\tilde{U}w)_{\eta\eta}|| \leqslant C_1||w|| + C_2||w_\eta|| + C_3||w_{\eta\eta}||,
$$

thus

$$
\frac{d}{dt}||w_{\eta\eta}|| \leqslant C_1||w|| + C_2||w_\eta|| + C_3||w_{\eta\eta}||.
\tag{3.34}
$$

The boundedness of $||w_{\eta\eta}||$ follows from Grönwall's inequality and assumption (3.26), and similarly for $||w_{\eta\eta\eta}||$. $||\alpha_I w_{\eta\eta}||$, $||\tilde{U}w_\eta||$ are also bounded. By Lemma 3.2, $||\partial_{z_1}\tilde{U}w|| \sim C\varepsilon^{\frac{3}{2}}||w||$. Using Grönwall's inequality on (3.31), one gets

$$
||\partial_{z_1}w|| \leq C_T,
$$

where C_T is a $O(1)$ constant, independent of ε. By induction, we obtain

$$
||\partial_{\mathbf{z}}^{\mathbf{k}}w|| \leq C_T,
$$

where $\partial_{\mathbf{z}}^{\mathbf{k}} = \partial_{z_1}^{k_1} \cdots \partial_{z_n}^{k_n}$. Therefore, we have shown Theorem 3.1. $\square$

4   Quantum and classical uncertainty

In this section we briefly discuss about quantum and classical uncertainty, and about the comparison between quantum and classical systems, for small values of the rescaled Planck's constant. For simplicity, we first consider the case with one degree of freedom, $x \in \mathbb{R}$, and scalar random variable z.

4.1   Moments and expectations

A quantum system is completely determined by its wave function ψ. For each realisation of the random variable z, the quantum system is described by $\psi(x, t, z)$.

The primary physical quantities of interest include the position density,

$$\rho(t, x, z) = |\psi(t, x, z)|^2,$$

and the current density,

$$j(t, x, z) = \varepsilon \operatorname{Im} \left(\overline{\psi}(t, x, z) \nabla \psi(t, x, z) \right).$$

Some quantities of interest to look at are the mean and standard deviation in z. In this way we can define the means:

$$\mathbb{E}[\rho](x, t) = \int \rho(x, t, z) \pi(z) \, dz, \quad \mathbb{E}[j](x, t) = \int j(x, t, z) \pi(z) \, dz \qquad (4.35)$$

and variance:

$$\mathbb{Var}[\rho](x, t) = \mathbb{E}[\rho^2] - \mathbb{E}[\rho]^2, \quad \mathbb{Var}[j](x, t) = \mathbb{E}[j^2] - \mathbb{E}[j]^2. \qquad (4.36)$$

The standard deviation will be computed as the square root of the variance:

$$\mathbb{SD}[\rho] = \sqrt{\mathbb{Var}[\rho]}, \quad \mathbb{SD}[j] = \sqrt{\mathbb{Var}[j]}.$$

For quantum systems we denote by $< h >=< \psi|h|\psi >$ the expectation value of observable h. Such a quantity will in general be a function of time and z. For example

$$< q > =< q > (t, z) =< \psi|\hat{q}|\psi >= \int \overline{\psi}(x, t, z) x \psi(x, t, z) \, dx,$$

$$< p > =< p > (t, z) =< \psi|\hat{p}|\psi >= -i\varepsilon \int \overline{\psi}(x, t, z) \psi_x(x, t, z) \, dx,$$

where $\hat{q} = x \cdot$ and $\hat{p} = -i\varepsilon \frac{\partial}{\partial x}$ denote, respectively, the position and momentum operators when the wave function ψ is in the space representation.

Because of the uncertainty in the parameter z, such quantities are random variables. It is possible to compute mean and variance of them as a function of time:

$$\mathbb{E}[< h >] = \int < h > (t, z) \pi(z) \, dz,$$

$$\mathbb{Var}[< h >] = \mathbb{E}((< h > - \mathbb{E}(< h >))^2) = \int (< h > - \mathbb{E}[< h >])^2 \pi(z) \, dz,$$

14

where h denotes, for example, q or p.

Notice that the average density $\mathbb{E}[\rho]$ and the average current $\mathbb{E}[j]$ can be used to compute an (ensemble) average particle position and momentum, since the two integration processes commute, i.e., for example, $\mathbb{E}[< x >] = < \mathbb{E}[x] >$. However, the same is not true for the variance. As we shall see, it is possible to consider the classical limit of $\mathbb{Var}[< x >]$, while is it hard to define such a limit for $\mathbb{Var}[\rho]$.

4.2 Classical limit

In classical mechanics, position and momentum of the particle follow Hamilton's equation

$$\dot{q} = \frac{\partial H}{\partial p}, \quad \dot{p} = -\frac{\partial H}{\partial q},$$

subject to some initial condition $q(0, z) = q_0(z)$, $p(0, z) = p_0(z)$. As in the quantum case, the uncertainty can be introduced at the level of the initial condition or at in the potential that defines the Hamiltonian:

$$H = \frac{p^2}{2m} + V(q, z),$$

where the random parameter z is distributed with a given density $\pi(z)$.

Position and momentum at a given time are therefore function of z as well: $q = q(t, z)$, $p = p(t, z)$. If such a density is known, then the probability distribution function (pdf) of the coordinate q can be found by classical techniques to find pdf of a function of a random variable. One which is commonly adopted in the physics community is given by

$$\mathcal{P}_q(x, t) = \int \delta(x - q(t, z))\pi(z)\, dz, \tag{4.37}$$

where δ denotes Dirac's delta, and the integral has to be interpreted in the usual distributional sense. This representation can be interpreted as follows: for each realization or the random variable, a classical particle can be seen as a singular particle density

$$\rho_c(x, t, z) = \delta(x - q(t, z)).$$

The probability distribution is then computed by weighting each value of the parameter with its probability density function, thus obtaining expression (4.37).

Assuming the function $q(t, z)$ is monotone in z, the integral can be easily computed by substitution, using the inverse function $z = z(t, q)$, yielding

$$\mathcal{P}_q(x) = \pi(z(t, x))|\partial z/\partial x|.$$

A suitable generalisation is possible in the case $q(t, z)$ is not monotone:

$$\mathcal{P}_q(x) = \sum_{z:q(t,z)=x} \frac{\pi(z)}{|\partial q(t, z)/\partial z|}. \tag{4.38}$$

Likewise, the mean current density distribution can be computed by smoothing the singular current corresponding to a single realization of the parameter z

$$j_c(x, t, z) = \rho_c(x, t, z)p(t, z)$$

by the pdf $\pi(z)$, obtaining

$$j_c(x, t) = \int \delta(x - q(t, z))p(t, z)\pi(z)\, dz.$$

Using the same argument, such current distribution can be computed as

$$j_c(x, t) = \sum_{z:q(t,z)=x} \frac{\pi(z)}{|\partial q(t, z)/\partial z|}p(t, z).$$

The situation with several degrees of freedom or with multivariate distribution is slightly different. Let us denote by d the number of degrees of freedom, and by m the number of random parameters. If $d = m$ then Equation (4.38) is still valid by interpreting $|\partial q(t, z)/\partial z|$ as the Jacobian of the transformation between z and q. If $d > m$, then in general the pdf will be proportional to a Dirac mass on a manifold of dimension $d - m$. If $d < m$ then in general the pdf will still be a function, which can be computed by integration on a manifold of dimension $m - d$. As an example we mention here the case $d = 1$, $m = 2$.

$$\mathcal{P}_q(x) = \sum_{\Gamma:q(t,z)=x} \int_{\Gamma} \frac{\pi(z)}{|\nabla_z q(t, z)|}\, d\Gamma, \tag{4.39}$$

where the sum is performed on all lines Γ such that $q(t, z) = x$.

Sometimes one is not interested in the computation of the space distribution of the particle density or the current density, but just in some moments, such as the mean and the variance. They can be computed as

$$\mathbb{E}[q] = \int q(t, z)\pi(z)\, dz, \quad \mathbb{E}[p] = \int p(t, z)\pi(z)\, dz,$$
$$\mathbb{Var}[q] = \mathbb{E}[q^2] - \mathbb{E}[q]^2, \quad \mathbb{Var}[p] = \mathbb{E}[p^2] - \mathbb{E}[p]^2.$$

5 Numerical Simulations

5.1 The stochastic collocation method

We now briefly review the gPC method [30]. In its stochastic Galerkin formulation, the gPC-SG approximation has been successfully applied to many stochastic physical and engineering problems, see for instance an overview [28, 15].

On the other hand, the stochastic collocation (SC) method [29, 7] is known as a popular choice for complex systems with uncertainties when reliable, well-established deterministic solvers exist. It is non-intrusive, so it preserves all features of the deterministic scheme,

and easy to parallelize [28, 22]. The basic idea is as follows. Let $\{\mathbf{z}_k\}_{k=1}^{N_z} \subset I_\mathbf{z}$ be the set of collocation nodes, N_z the number of samples. For each fixed individual sample $\mathbf{z}_k$, $k = 1, \ldots, N_z$, one applies the deterministic solver to the deterministic equations as in [26], obtains the solution ensemble for a general function $f(t, x, \mathbf{z})$, $f_k(t, x) = f(t, x, \mathbf{z}_k)$, then adopts an interpolation approach to construct a gPC approximation

$$f(t, x, \mathbf{z}) = \sum_{k=1}^{N_z} f_k(t, x) l_k(\mathbf{z}),$$

where $l_k(\mathbf{z})$ depends on the construction method. The Lagrange interpolation is used here by choosing $l_k(\mathbf{z}_i) = \delta_{ik}$. With samples $\{\mathbf{z}_k\}$ and corresponding weights $\{\nu_k\}$ chosen from the quadrature rule, the integrals in $\mathbf{z}$ are approximated by

$$\int_{I_\mathbf{z}} f(t, x, \mathbf{z}) \pi(\mathbf{z}) d\mathbf{z} \approx \sum_{k=1}^{N_z} f_k(t, x) \nu_k, \tag{5.40}$$

where

$$\nu_k = \int_{I_\mathbf{z}} l_k(\mathbf{z}) \pi(\mathbf{z}) d\mathbf{z}.$$

Considering the structure complexity of the deterministic solver developed in [26, 27], we choose the SC rather than gPC-SG in this project due to its simplicity and efficiency in implementation. In numerical simulation, we need to sample the Gaussian wave packet parameters and the w function, while in solution construction, we are interested in the wave equation as well as physical observables which are nonlinear transforms of the wave equation. In this sense, the stochastic collocation method offers great flexibility in computing averages of various quantities in the random space. We will introduce below how the SC and GWPT method are combined in our numerical implementation.

5.2 Numerical implementation

We first briefly review the meshing strategy for the GWPT based method in x and t when the random variables are not present. Recall that the GWPT maps the semi-classical Schrödinger equation to the ODE system for the wave packet parameters and the w equation. In numerical simulation, we denote the time step for the ODE system by Δt_1, the time step for the w equation by Δt_2 and the spatial grid size for the w equation by $\Delta \eta$. We introduce a spatial mesh in $\mathbf{x}$ with grid size Δx, in the final reconstruction step for ψ.

Since the w equation does not produce $O(\varepsilon)$ scaled oscillations, Δt_2 and $\Delta \eta$ can be chosen independently of ε. The phase term in the GWPT is computed by solving the ODE system of the Gaussian wave packet parameters, where the ODE system does not contain stiff terms due to ε. However, the numerical error in solving the phase term is magnified by a factor of ε^{-1} when constructing the wave function, thus we often need to take Δt_1 to be $O(\varepsilon^{1/k})$, where k denotes the accuracy order of the ODE solver. Finally, Δx used in the reconstruction step also needs to be $O(\varepsilon)$ in order to resolve small oscillations in the wave function. The interested readers may refer to [26, 27] for a more detailed discussion.

We now discuss the sampling strategy for each step of the numerical implementation in the random space. Three sets of collocation points in $\mathbf{z}$ are used in our numerical tests:

- number of points to solve the ODEs for the wave packet parameters given by the following system (5.41): $N_{z,1}$,
  At each collocation point $\mathbf{z}_k$ $(k = 1, \cdots, N_{z,1})$, we have

$$
\begin{cases}
\partial_t q(t, \mathbf{z}_k) = p(t, \mathbf{z}_k), \\
\partial_t p(t, \mathbf{z}_k) = -\nabla V(q, \mathbf{z}_k), \\
\partial_t \alpha(t, \mathbf{z}_k) = -2(\alpha(t, \mathbf{z}_k))^2 - \frac{1}{2}\nabla\nabla V(q, \mathbf{z}_k), \\
\partial_t \gamma(t, \mathbf{z}_k) = \frac{1}{2}(p(t, \mathbf{z}_k))^2 - V(q, \mathbf{z}_k) + i\varepsilon \operatorname{Tr}(\alpha_R(t, \mathbf{z}_k)).
\end{cases}
\tag{5.41}
$$

- number of points to solve the w equation (3.30): $N_{z,2}$,

- number of points to reconstruct ψ: $N_{z,3}$.

The sets of mesh points $N_{z,1}$, $N_{z,2}$ and $N_{z.3}$ used above are denoted by M_1, M_2 and M_3 respectively. The cardinality of the set M_j is $N_{z,j}$ $(j = 1, 2, 3)$.

After computing the wave packet parameters in (5.41) at the mesh points M_1 in the z direction, cubic spline interpolation is used to get the values of these parameters at the mesh points M_2, which prepares us to update w by solving (3.30) in time at the same mesh points of z, i.e., M_2. In the reconstruction step, for each $\mathbf{z}_k$,

$$
\psi(x, t, \mathbf{z}_k) = \widetilde{w}(\xi, t, \mathbf{z}_k) \exp\left(i\left(\xi^T \alpha_R \xi + p^T \xi + \gamma\right)/\varepsilon\right),
\tag{5.42}
$$

with $\xi = x - q$ and $\mathbf{z}_k \in M_3$. Cubic spline interpolation is used to obtain values of wave packet parameters from M_1 to M_3, and values of w from M_2 to M_3, which is the reconstruction mesh points. Now we have the values of $\psi = \psi(x, t, \mathbf{z}_k)$ at mesh points $\{\mathbf{z}_k\}$, for $k = 1, \cdots, N_{z,3}$. Finally, in order to plot the solution ψ and its physical quantities of interest at a set of fixed physical location, denoted by X_0, cubic spline interpolation is used again. Note that in practice one does not need to reconstruct ψ: the observables, such as the expectation values for position and momentum, can be computed directly from w. See Section 2.4 in [26].

We now discuss the sampling strategy in $\mathbf{z}$ for the GWPT method. Although the parameter system (5.41) does not have ε oscillations in $\mathbf{z}$, the numerical error in the parameters are magnified by ε^{-1} when reconstructing the wave function as in (5.42). Therefore, one expects that $N_{z,1}$ should depend on ε in order to obtain accurate approximation of the wave function, and the dependence is related to the ODE solver used for the parameter system. Due to the regularity property of the w equation in $\mathbf{z}$, we expect that we can take ε independent numbers of collocation points, and thus it suffices to take $N_{z,2} = O(1)$. Clearly, we need to take $N_{z,3} = O(\varepsilon^{-1})$ to resolve the oscillation in $\mathbf{z}$ in the wave function reconstruction.

We remark that, although in the sampling strategy in z we require $N_{z,1}$ and $N_{z,3}$ to be ε dependent, it does not cause much computational burdens, because the $N_{z,1}$ collocation points are only used to the ODE system and the $N_{z,3}$ collocation points are used in the

final step. On the other hand, *in the most expensive part, solving the w equation in time, we only use ε independent numbers of collocation points. Hence, such sampling strategy is desired for the sake of computational efficiency.*

Finally, considering that certain physical observables, such as position density and flux density can be obtained directly from the w function, then $N_{z,1}$ is expected to be independent of ε if one is only interested to capture the correct physical observables. This argument will be verified numerically in the tests of Section 5.3.

5.2.1 Numerical observables

With the obtained $\psi(t, X, \mathbf{z}_k)$ and the corresponding weights $\{\nu_k\}$ for $k = 1, \cdots, N_{z,3}$, chosen from the quadrature rule, one can approximate the integral given by (2.15),

$$||\psi||^2_\Gamma = \int_{I_\mathbf{z}} \int |\psi(t, \mathbf{x}, \mathbf{z})|^2 \, d\mathbf{x}\pi(\mathbf{z})d\mathbf{z} \approx \sum_{k=1}^{N_{z,3}} \sum_{i=1}^{N_x} |\psi(x_i, \mathbf{z}_k)|^2 \Delta x \, \nu_k. \qquad (5.43)$$

To be consistent with the Γ-norm we defined in (2.15), we first denote the $L^1(x)$ norm of $j(t, x, \mathbf{z}_k)$ by $\widetilde{j}(t, \mathbf{z}_k)$ for $k = 1, \cdots N_{z,3}$,

$$\widetilde{j}(t, \mathbf{z}_k) = \varepsilon \int \mathrm{Im}\left(\overline{\psi}(t, x, \mathbf{z}_k)\nabla\psi(t, x, \mathbf{z}_k)\right) dx \approx \sum_{i=1}^{N_x} \varepsilon \left(\overline{\psi}(t, x_i, \mathbf{z}_k)\nabla\psi(t, x_i, \mathbf{z}_k)\right) \Delta x,$$

then get $\mathbb{E}(\widetilde{j})$, $\mathbb{V}\mathrm{ar}(\widetilde{j})$ and $\mathbb{SD}(\widetilde{j})$:

$$\mathbb{E}(\widetilde{j}) \approx \sum_{k=1}^{N_{z,3}} \widetilde{j}(t, \mathbf{z}_k)\nu_k, \qquad \mathbb{V}\mathrm{ar}(\widetilde{j}) = \mathbb{E}(\widetilde{j}^2) - (\mathbb{E}(\widetilde{j}))^2, \qquad \mathbb{SD}(\widetilde{j}) = \sqrt{\mathbb{V}\mathrm{ar}(\widetilde{j})}. \qquad (5.44)$$

5.2.2 Definition of errors

The error in ψ is computed by comparing ψ with the reference solutions obtained from the second-order direct splitting method, where a sufficiently large number of collocation points $N_{z,4}$ is used. Denote the set of mesh points by M_4. The error is measured under the averaged norm (2.15), with the discretized form of the approximation shown in (5.43). More precisely, we use the relative error defined by

$$\mathrm{Er}[\psi] = \frac{||\psi_G - \psi_D||_\Gamma}{||\psi_D||_\Gamma}, \qquad (5.45)$$

where ψ_G represents the solution obtained by the GWPT method, and ψ_D represents the one obtained from the direct splitting method. To compute $||\psi_G - \psi_D||_\Gamma$ in (5.45), one needs values of both $\psi_G(t, X_0, z_j)$ and $\psi_D(t, X_0, z_j)$ at the same set of mesh points of z, denoted by M_5 and the number of collocation points $N_{z,5}$. Thus

$$||\psi_G - \psi_D||^2_\Gamma \approx \sum_{j=1}^{N_{z,5}} \sum_{i=1}^{N_x} |\psi_G(x_i, z_j) - \psi_D(x_i, z_j)|^2 \Delta x \, \nu_j.$$

Here one needs to find the interpolated values of Ψ_G and Ψ_D corresponding to the mesh points M_5, from mesh points M_3 and M_4 respectively. We let $M_5 = M_3$ for simplicity. All the interpolation in z space refers to the spline interpolation.

To quantify the errors in mean and standard deviation of the current density, we use

$$\mathrm{Er}_1[j] = \left| \frac{\mathbb{E}(\widetilde{j}_G - \widetilde{j}_D)}{\mathbb{E}(\widetilde{j}_D)} \right|, \qquad \mathrm{Er}_2[j] = \left| \frac{\mathbb{SD}(\widetilde{j}_G - \widetilde{j}_D)}{\mathbb{SD}(\widetilde{j}_D)} \right|, \tag{5.46}$$

where $\mathbb{E}$ and $\mathbb{SD}$ are calculated by using (5.44). Note that the mass at each collocation point $\mathbf{z}_k$ namely $\int |\psi(t, x, \mathbf{z}_k)|^2 dx$ is a conserved quantity with respect to time and a constant. Thus it is not interesting to compute the relative errors of ρ in terms of the Γ-norm as that for j.

5.3   Numerical Tests

Part I: Relation between $N_{z,1}$, $N_{z,2}$, $N_{z,3}$, $N_{z,4}$ and ε

We know from the deterministic problem in [26] that all the stiffness in time and space of the original Schrödinger equation for ψ associated with very small values of ε is essentially been removed in the equation for $w(\eta, t)$ by the GWP transform. Since we proved in subsection 3.2 that w equation is not oscillatory in z, all the orders of z-derivatives of w have a uniform upper bound, thus the number of collocation points used to solve w, namely $N_{z,2}$ is expected to be independent of ε.

In Part I of the numerical tests, we will demonstrate for sufficiently large $N_{z,1}$ and $N_{z,3}$ that are proportional to $1/\varepsilon$ and $1/\sqrt{\varepsilon}$ respectively, one can choose $N_{z,2}$ *uniformly* with respect to ε.

We put uncertainty in the potential function in Test (a1)–(a3).

Test (a1)

In this test, we assume z a one-dimensional random variable that follows a uniform distribution on $[-1, 1]$. Consider the spatial domain $x \in [-\pi, \pi]$ with periodic boundary conditions. The initial data of ψ is

$$\psi(x, 0) = A \exp\big[(i/\varepsilon)\big(\alpha_0(x - q_0)^2 + p_0(x - q_0)\big)\big], \tag{5.47}$$

where $q_0 = \pi/2, p_0 = 0, \alpha_0 = i$. We name Test (a1-i) and Test (a1-ii) with different potentials:

$$\textbf{Test (a1-i)} \quad V(x, z) = (1 + 0.95z)x^2,$$

$$\textbf{Test (a1-ii)} \quad V(x, z) = (1 - \cos(x))(1 + 0.9z).$$

Let $\Delta t_1 = 0.01$, $\Delta\eta = 0.3125$ in the w equation, and $\Delta t_2 = 2.5 \times 10^{-4}$ in the ODEs for solving the parameters p, q, α, γ. $\Delta t = 1/600$ and $\Delta x = 2\pi/9600$ in the reference solutions. $T = 1$ in Test (a1)–(a3).
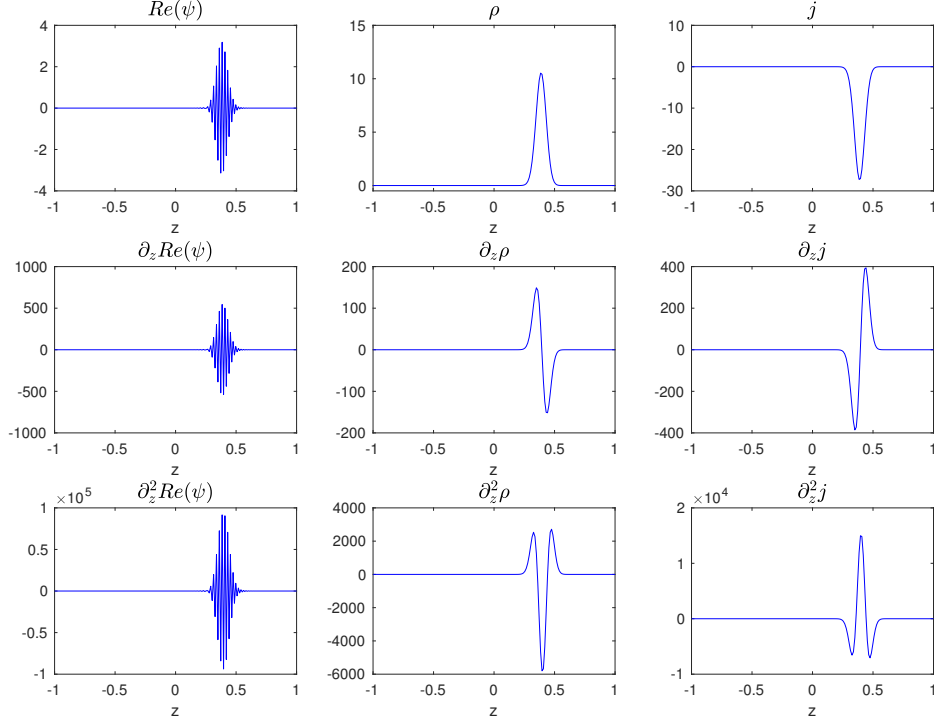
Figure 1: Test (a1-i), $\varepsilon = 1/256$. Plot at $x = -0.1316$, $T = 1$.

In Test (a1-i), we choose the random potential $V(x, z) = (1 + 0.95z)x^2$. The reason we choose potential function quadratic in x is that the form of exact solution (2.17) is known in this case. Solutions of $\mathrm{Re}(\psi)$, ρ, j as a function of z at some physical location x are plotted in Figure 1. The plot indicates that 1) the behaviors of ψ or z-derivatives of ψ are much more oscillatory than that of ρ and j; 2) regarding the relations between the amplitude of $\mathrm{Re}(\psi)$, ρ, j and their first and second order partial z-derivatives, numerical results seem to suggest that $\mathrm{Re}(\psi)$ increases by $O(1/\varepsilon)$ each time we differentiate it, and ρ, j tend to increase by $O(1/\sqrt{\varepsilon})$ as the order of z-derivative increases.

We now compare the trend of maximum values of the z-derivatives of ψ and w with respect to different ε:

ε	$\frac{1}{32}$	$\frac{1}{64}$	$\frac{1}{128}$	$\frac{1}{256}$	$\frac{1}{512}$
$\max \partial_z Re(\psi)$	40.5971	96.1058	228.0143	541.3633	1.2843e+03
$\max \partial_z Re(w)$	0.0618	0.0521	0.0439	0.0370	0.0313

Table 1: Test (a1-ii). Comparison of $\max \partial_z Re(\psi)$ and $\max \partial_z Re(w)$.

21

One can observe from Table 1 that $\max \partial_z \mathrm{Re}(\psi)$ increase much more rapidly than $\max \partial_z \mathrm{Re}(w)$, the former doubles its values as ε decreases to half smaller, the latter slightly changes its values. This demonstrates that while ψ is highly oscillatory in the random space, w is smooth in z, and it guides us to choose the following number of collocation points: take sufficiently large $N_{z,1} = N_{z,3} = N_{z,4} = 500$ and $N_{z,2} = 32$ in Test (a1)–(a3).
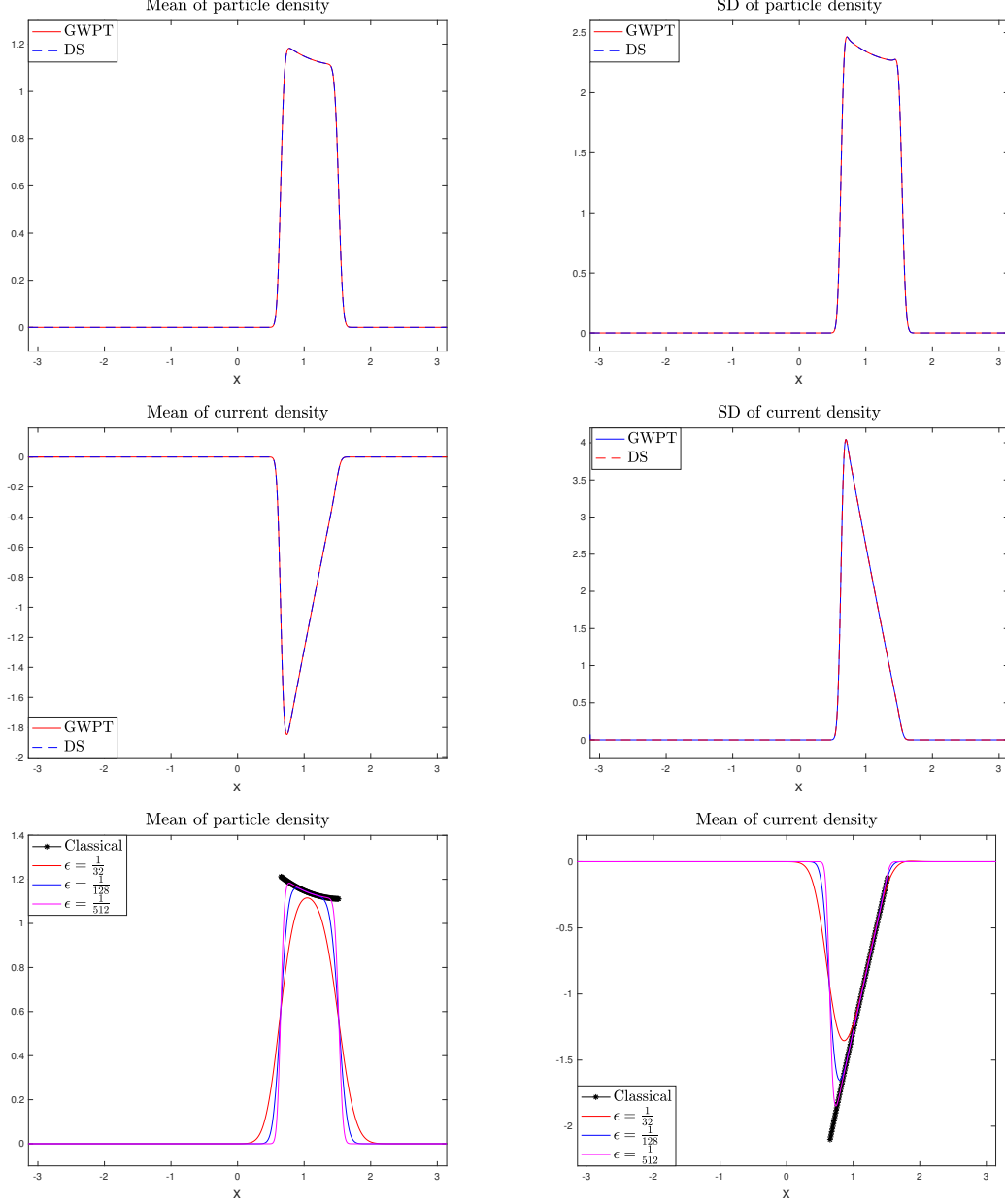

Figure 2: Test (a1-ii). Comparison of GWPT, DS and Classical method. $\varepsilon = \frac{1}{512}$ for the first two rows.

ε	$\mathrm{Er}[\psi]$	$\mathrm{Er}_1[j]$	$\mathrm{Er}_2[j]$
$\frac{1}{32}$	$2.9968e-05$	$3.1235e-07$	$1.0328e-06$
$\frac{1}{64}$	$3.2442e-05$	$3.6868e-07$	$9.5517e-07$
$\frac{1}{128}$	$3.1316e-05$	$1.5865e-07$	$4.2628e-07$
$\frac{1}{256}$	$3.7924e-05$	$1.6370e-07$	$3.8290e-07$

Table 2: Test (a1-ii). Error of ψ and mean and standard deviation of j with respect to different ε.

$N_{z,2}$	$\mathrm{Er}[\psi]$	$\mathrm{Er}_1[j]$	$\mathrm{Er}_2[j]$
2	0.0013	$3.8978e-07$	$5.4256e-05$
4	$1.7219e-05$	$7.4463e-09$	$3.0955e-06$
8	$1.3416e-07$	$6.4828e-09$	$4.1892e-08$
16	$7.5591e-09$	$4.5480e-10$	$1.4003e-09$
32	$4.9371e-10$	$2.9899e-11$	$8.8615e-11$

Table 3: Test (a1-ii), $\varepsilon = 1/256$. Relative errors for solutions computed by increasing $N_{z,2}$.

Test (a2)–(a3) use the same initial data of ψ as shown in (5.47).

Test (a2) Let z follow the normal Gaussian distribution, with the random potential

$$V(x,z) = (1 - \cos(x))(1 + 0.9z).$$

ε	$\mathrm{Er}[\psi]$	$\mathrm{Er}_1[j]$	$\mathrm{Er}_2[j]$
$\frac{1}{32}$	4.8231×10^{-05}	2.4561×10^{-07}	1.8024×10^{-05}
$\frac{1}{64}$	3.0519×10^{-05}	2.3575×10^{-07}	8.7407×10^{-06}
$\frac{1}{128}$	3.1520×10^{-05}	2.3147×10^{-07}	6.1686×10^{-06}
$\frac{1}{256}$	3.7955×10^{-05}	2.1877×10^{-07}	5.3444×10^{-06}

Table 4: Test (a2). Error of ψ and mean and standard deviation of j with respect to different ε.

Test (a3) We let

$$V(x,z) = (1 - \cos(x))(1 + \varepsilon z), \tag{5.48}$$

with z followed the normal Gaussian distribution.

ε	$\mathrm{Er}[\psi]$	$\mathrm{Er}_1[j]$	$\mathrm{Er}_2[j]$
$\frac{1}{32}$	$2.9898e-05$	$4.9752e-08$	$8.3984e-07$
$\frac{1}{64}$	$3.2074e-05$	$1.4983e-07$	$7.9849e-07$
$\frac{1}{128}$	$3.1146e-05$	$5.9345e-08$	$3.5599e-07$
$\frac{1}{256}$	$3.7461e-05$	$8.1869e-08$	$3.3017e-07$

Table 5: Test (a3). Error of ψ and mean and standard deviation of j with respect to different ε.

In Figure 2, we see that solutions of the mean and standard deviation of ρ and j obtained from GWPT match well with the reference solutions calculated from the time splitting spectral method [2]. In the last row of Figure 2, we compare the mean of ρ and j obtained from GWPT for several values of ε (lines) with the mean density and current obtained by classical mechanics (dots). One observes a tendency of convergence of the solutions of GWPT to che classical case as ε becomes smaller from $\varepsilon = \frac{1}{32}$ and $\varepsilon = \frac{1}{128}$ to $\varepsilon = \frac{1}{512}$. However, it is yet to be specified the precise description of the weak convergence, which remains a difficult question, as discussed at the end of subsection 2.1.

In Tables 2, 4 and 5, one observes a uniform accuracy for ψ and j with respect to different small values of ε. Thus we conclude that in order to capture ψ and j, ε-independent $N_{z,2}$ ($N_{z,2} = 32$) can be used for all small ε, by putting $N_{z,1}$, $N_{z,3}$ and $N_{z,4}$ sufficiently large. In Table 3, fixing ε, we see a fast spectral convergence of relative errors between using $N_{z,2}$ and $2N_{z,2}$ for ψ and j, which indicates again that small ε-independent $N_{z,2}$ can be chosen to obtain accurate values of ψ and j.

In the following Test (b) and Test (c), we let the initial data for ψ depend on the random variable z that follows a uniform distribution on $[-1, 1]$. Let $N_{z,1} = N_{z,3} = N_{z,4} = 500$, $N_{z,2} = 32$ in Test (b) and Test (c).

Test (b) Let

$$V(x) = 1 - \cos(x), \qquad \psi(x, 0, z) = A \exp\big[(i/\varepsilon)\big(\alpha_0(x - q_0)^2 + p_0(x - q_0)\big)\big].$$

Here we assume q_0 random,

$$q_0 = \frac{\pi}{2}(1 + 0.5z), \qquad p_0 = 0, \qquad \alpha_0 = i.$$

ε	$\mathrm{Er}[\psi]$	$\mathrm{Er}_1[j]$	$\mathrm{Er}_2[j]$
$\frac{1}{32}$	$1.1114e-04$	$2.5535e-07$	$1.5763e-06$
$\frac{1}{64}$	$3.1764e-05$	$7.8356e-08$	$2.4191e-06$
$\frac{1}{256}$	$5.8151e-05$	$1.5883e-07$	$1.9183e-06$

Table 6: Test (b). Error of ψ and mean and standard deviation of j with respect to different ε. $T = 1$.

24

Test (c) Let

$$V(x) = 1 - \cos(x), \qquad \psi(x, 0, z) = A \exp\left[(i/\varepsilon)\left(\alpha_0(x - q_0)^2 + p_0(x - q_0)\right)\right],$$

with q_0, p_0 depend on z,

$$q_0 = \frac{\pi}{2}(1 + 0.5z), \qquad p_0 = 0.5z, \qquad \alpha_0 = i.$$

ε	$\mathrm{Er}[\psi]$	$\mathrm{Er}_1[j]$	$\mathrm{Er}_2[j]$
$\frac{1}{32}$	$1.6159e-04$	$1.8413e-07$	$5.9809e-07$
$\frac{1}{64}$	$2.5781e-05$	$1.1032e-07$	$1.9014e-07$
$\frac{1}{256}$	$2.5840e-05$	$1.1882e-08$	$1.3267e-07$

Table 7: Test (c). Error of ψ and mean and standard deviation of ρ and j with respect to different ε. $T = 0.5$.

Table 6 and Table 7 give the same conclusion as Tests (a1)–(a3), that is, ε-independent $N_{z,2}$ (and sufficient large $N_{z,1}$, $N_{z,3}$, $N_{z,4}$) can be chosen to get accurate ψ and j.

Now we perform a two-dimensional random variable test:

Test (d) Let the random potential be

$$V(x, z) = (1 - \cos(x))(1 + 0.2z_1 + 0.7z_2), \tag{5.49}$$

where z_1, z_2 both follow uniform distributions on $[-1, 1]$. The initial data of ψ is given by (5.47). $\varepsilon = 0.1$. Use $N_{z,1} = N_{z,2} = N_{z,3} = N_{z,4} = 32$. Solutions and errors at time $T = 1$ are shown in Figure 3 below.
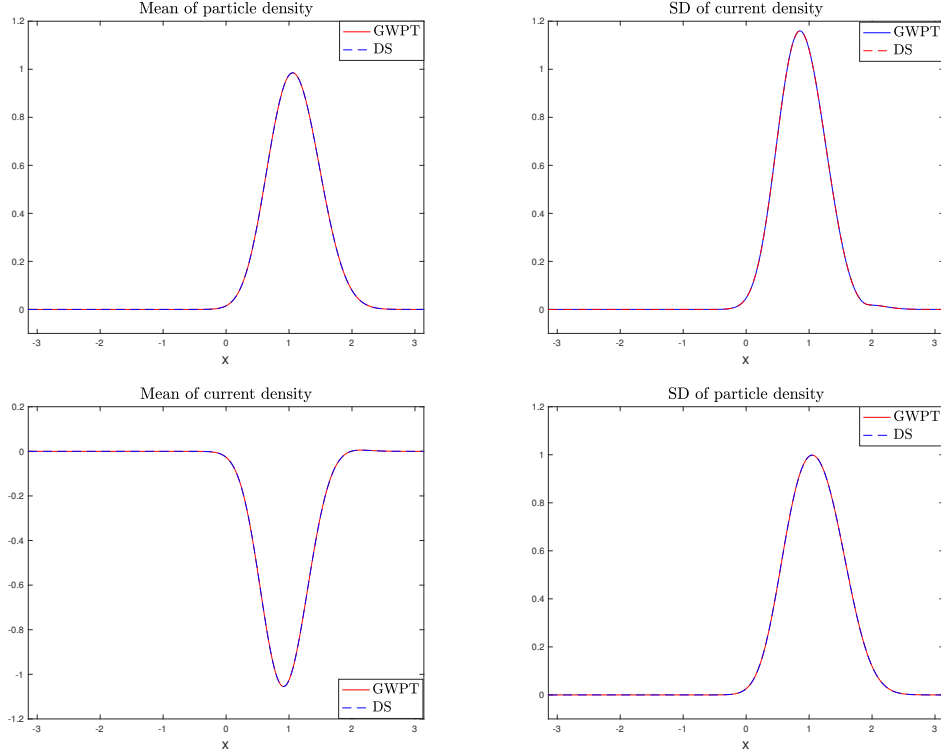
$\text{Er}[\psi]$	$\text{Er}_1[j]$	$\text{Er}_2[j]$
$4.2501e-04$	$1.2864e-06$	$1.7532e-06$

Figure 3: Test (d). Comparison of GWPT with DS.

Figure 3 shows that we can capture accurately the mean and standard deviation of ρ and j when the random potential has a two-dimensional random variable. Since ε in this test is not so small, $N_{z,1}$, $N_{z,2}$, $N_{z,3}$ and $N_{z,4}$ do not have to be very large.

Part II: Comparison between different perturbations in $V(x,z)$ and an error vs. time plot

We compare three different orders of perturbations, using ε-independent $N_{z,1}$, $N_{z,2}$, $N_{z,3}$ and ε-dependent $N_{z,4}$.

We first introduce Test (a4) and compare it with Test (a2) and Test (a3).

Test (a4) We assume that z follows the normal Gaussian distribution, and the random potential given by

$$V(x,z) = (1 - \cos(x))(1 + \sqrt{\varepsilon}z). \tag{5.50}$$

If one only needs the information of macroscopic quantities such as the current density,

26

whose errors are measured by $\mathrm{Er}_1[j]$ and $\mathrm{Er}_2[j]$ in (5.46), then the collocation points $N_{z,1}$, $N_{z,2}$, $N_{z,3}$ used in the GWPT method can be chosen independently of small ε.

From Tables 8, 9 and 10 below, in which $N_{z,1} = N_{z,2} = N_{z,3} = 32$, $N_{z,4} = 500$ and $T = 1$. Recall that Test (a2) has a $(1 + 0.9z)$ perturbation in $V(x, z)$; Test (a3) has a $(1 + \varepsilon z)$ perturbation in $V(x, z)$, and Test (a4) has a $(1 + \sqrt{\varepsilon}z)$ perturbation in $V(x, z)$. One observes that errors for the mean and standard deviation of j in the three tests are uniformly small with respect to different values of small ε. This is usually not the case for ψ, whose errors $\mathrm{Er}[\psi]$ increase for smaller values of ε, because of its increasingly oscillatory behavior. However, the errors of ψ in Table 8 are shown to be much smaller than that in Tables 9 and 10, which indicates that if the random perturbation of the potential is relatively small, e.g., of $O(\varepsilon)$ perturbation in the test of Table 8 compared to $O(\sqrt{\varepsilon})$ and $O(1)$ perturbation in the tests of Table 9 and 10 respectively, then ε-independent $N_{z,1}$, $N_{z,2}$, $N_{z,3}$ can be used to capture ψ accurately.

ε	$\mathrm{Er}[\psi]$	$\mathrm{Er}_1[j]$	$\mathrm{Er}_2[j]$
$\frac{1}{32}$	$2.8859e-05$	$9.5081e-08$	$4.1857e-07$
$\frac{1}{64}$	$2.9239e-05$	$8.4372e-09$	$3.7980e-07$
$\frac{1}{128}$	$3.1145e-05$	$5.9345e-08$	$3.5599e-07$
$\frac{1}{256}$	$3.7461e-05$	$8.1869e-08$	$3.3013e-07$

Table 8: Test (a3). Error of ψ and mean and standard deviation of j with respect to different ε.

ε	$\mathrm{Er}[\psi]$	$\mathrm{Er}_1[j]$	$\mathrm{Er}_2[j]$
$\frac{1}{32}$	$5.0359e-04$	$3.2411e-08$	$5.8941e-07$
$\frac{1}{64}$	0.0020	$6.2931e-08$	$5.3575e-07$
$\frac{1}{128}$	0.0093	$1.0983e-07$	$5.0308e-07$
$\frac{1}{256}$	0.0535	$1.2743e-07$	$4.5854e-07$

Table 9: Test (a4). Error of ψ and mean and standard deviation of j with respect to different ε.

ε	$\mathrm{Er}[\psi]$	$\mathrm{Er}_1[j]$	$\mathrm{Er}_2[j]$
$\frac{1}{32}$	0.5842	$4.2896e-07$	$1.8105e-05$
$\frac{1}{64}$	1.9324	$4.6665e-07$	$8.8690e-06$
$\frac{1}{128}$	1.8047	$4.7258e-07$	$6.4676e-06$
$\frac{1}{256}$	1.6294	$4.1936e-07$	$4.6450e-06$

Table 10: Test (a2). Error of ψ and mean and standard deviation of j with respect to different ε.

part (iv):   Semi-log error plot vs. time

T	$\mathrm{Er}[\psi]$	$\mathrm{Er}_1[j]$	$\mathrm{Er}_2[j]$
1	$3.9592e-05$	$1.9887e-07$	$7.6387e-07$
$2^{1/2}$	$6.4139e-05$	$1.1964e-06$	$3.5285e-06$
2	$6.3926e-05$	$6.5872e-07$	$3.9316e-06$
$2^{3/2}$	$4.2088e-04$	$3.9568e-06$	$4.9694e-06$
4	$9.0106e-05$	$3.1581e-06$	$2.6140e-06$
$2^{5/2}$	$8.2447e-04$	$1.6763e-06$	$3.6021e-05$
8	0.0037	$1.1940e-05$	$3.0379e-04$

Table 11: Test (a4). Error of ψ and mean and standard deviation of j with respect to different time. $\varepsilon = 1/128$.
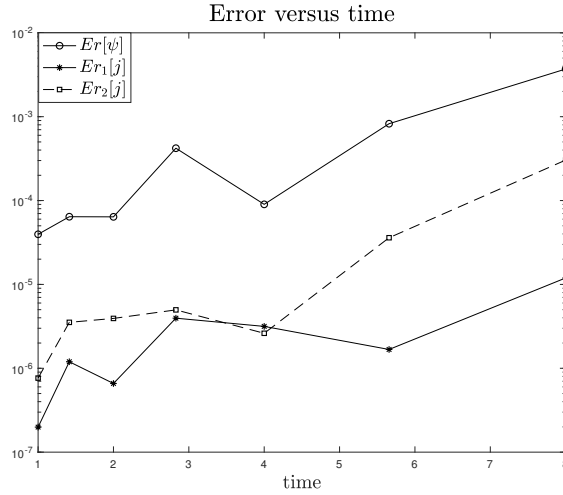

Figure 4: A semi-log plot of the errors versus time shown in Table 11.

In Table 11, we compute the errors of ψ, and mean and standard deviation of j with respect to different output time, with a corresponding semi-log plot shown in Figure 4. One can observe that the overall trend of all the errors increase as time becomes longer. This trend is similar as that in the counterpart deterministic problem [26].

6   Conclusion and future work

In this paper, we consider random potential or initial data in the semi-classical Schrödinger equation. Based on the Gaussian wave packet transform numerical method studied for the deterministic problem in [26], we adopt the stochastic collocation method to numerically

compute the Schrödinger equation with random inputs. We analyze how the number of collocation points needed at each step depends on the Planck constant ε, according to regularity analyses of the solution ψ and w in the random space. A variety of numerical experiments demonstrate our arguments and efficiency of the proposed numerical method.

In the future, we propose to work on high-dimensional random variable test and develop efficient numerical solvers. Multidimensional physical space was considered in [27], and we expect to study the counterpart problem with uncertainties. In [32], the semi-classical Schrödinger equation in the presence of electromagnetic field was reformulated by the Gaussian wave packets transform. It is interesting to consider random electromagnetic field and extend the numerical method studied in [32] to the random case.

References

[1] G. Bal, A. Fannjiang, G. Papanicolaou, and L. Ryzhik, *Radiative transport in a periodic structure*, J. Statist. Phys., 95 (1999), pp. 479–494.

[2] W. Bao, S. Jin, and P. A. Markowich, *On time-splitting spectral approximations for the Schrödinger equation in the semiclassical regime*, J. Comput. Phys., 175 (2002), pp. 487–524.

[3] J. Chen, J.-G. Liu, and Z. Zhou, *On a Schrödinger-Landau-Lifshitz system: variational structure and numerical methods*, Multiscale Model. Simul., 14 (2016), pp. 1463–1487.

[4] N. Crouseilles, S. Jin, M. Lemou, and L. Liu, *Nonlinear geometric optics based multiscale stochastic Galerkin methods for highly oscillatory transport equations with random inputs*, preprint, (2017).

[5] E. Faou, V. Gradinaru, and C. Lubich, *Computing semiclassical quantum dynamics with Hagedorn wavepackets*, SIAM J. Sci. Comput., 31 (2009), pp. 3027–3041.

[6] P. Gérard, P. A. Markowich, N. J. Mauser, and F. Poupaud, *Erratum: "Homogenization limits and Wigner transforms" [Comm. Pure Appl. Math.* **50** *(1997), no. 4, 323–379; MR1438151 (98d:35020)]*, Comm. Pure Appl. Math., 53 (2000), pp. 280–281.

[7] M. D. Gunzburger, C. G. Webster, and G. Zhang, *Stochastic finite element methods for partial differential equations with random input data*, Acta Numerica, 23 (2014), pp. 521–650.

[8] G. A. Hagedorn, *Raising and lowering operators for semiclassical wave packets*, Ann. Physics, 269 (1998), pp. 77–104.

[9] E. J. Heller, *Time dependent variational approach to semiclassical dynamics*, J. Chem. Phys., 64 (1976), pp. 63–73.

[10] S. Jin, P. Markowich, and C. Sparber, *Mathematical and computational methods for semiclassical Schrödinger equations*, Acta Numer., 20 (2011), pp. 121–209.

[11] S. Jin, H. Wu, and X. Yang, *Semi-Eulerian and high order Gaussian beam methods for the Schrödinger equation in the semiclassical regime*, Commun. Comput. Phys., 9 (2011), pp. 668–687.

[12] S. Jin and Z. Zhou, *A semi-Lagrangian time splitting method for the Schrödinger equation with vector potentials*, Commun. Inf. Syst., 13 (2013), pp. 247–289.

[13] K. Kay, *Integral expressions for the semi-classical time-dependent propagator*, J. Chem. Phys., 100 (1994), pp. 4377–4392.

[14] ——, *The Herman-Kluk approximation: derivation and semiclassical corrections*, Chem. Phys., 322 (2006), pp. 3–12.

[15] O. P. Le Maître and O. M. Knio, *Spectral methods for uncertainty quantification*, Scientific Computation, Springer, New York, 2010. With applications to computational fluid dynamics.

[16] S.-Y. Lee and E. J. Heller, *Exact time dependent wave packet propagation: Application to the photodissociation of methyl iodide*, The Journal of Chemical Physics, 76 (1982), pp. 3035–3044.

[17] P.-L. Lions and T. Paul, *Sur les mesures de Wigner*, Rev. Mat. Iberoamericana, 9 (1993), pp. 553–618.

[18] J. Lu and X. Yang, *Convergence of frozen Gaussian approximation for high-frequency wave propagation*, Comm. Pure Appl. Math., 65 (2012), pp. 759–789.

[19] J. Lu and Z. Zhou, *Improved sampling and validation of frozen gaussian approximation with surface hopping algorithm for nonadiabatic dynamics*, J. Chem. Phys., 145 (2016), p. 4109.

[20] J. Lu and Z. Zhou, *Frozen Gaussian approximation with surface hopping for mixed quantum-classical dynamics: a mathematical justification of fewest switches surface hopping algorithms*, Math. Comp., 87 (2018), pp. 2189–2232.

[21] Z. Ma, Y. Zhang, and Z. Zhou, *An improved semi-Lagrangian time splitting spectral method for the semi-classical Schrödinger equation with vector potentials using NUFFT*, Appl. Numer. Math., 111 (2017), pp. 144–159.

[22] F. Nobile, R. Tempone, and C. G. Webster, *A sparse grid stochastic collocation method for partial differential equations with random input data*, SIAM J. Numer. Anal., 46 (2008), pp. 2309–2345.

[23] G. Papanicolaou and L. Ryzhik, *Waves and transport*, IAS/PARK CITY Mathematics Series, L. Caffarelli and Weinan E editors, AMS, 5 (1998), pp. 305–382.

[24] J. Qian and L. Ying, *Fast multiscale Gaussian wavepacket transforms and multiscale Gaussian beams for the wave equation*, Multiscale Model. Simul., 8 (2010), pp. 1803–1837.

[25] J. Ralston, *Gaussian beams and the propagation of singularities*, in Studies in partial differential equations, vol. 23 of MAA Stud. Math., Math. Assoc. America, Washington, DC, 1982, pp. 206–248.

[26] G. Russo and P. Smereka, *The Gaussian wave packet transform: Efficient computation of the semi-classical limit of the Schrödinger equation. Part 1: a formulation and the one dimensional case*, Journal of Computational Physics, 233 (2013), pp. 192–209.

[27] ———, *The Gaussian wave packet transform: efficient computation of the semi-classical limit of the Schrödinger equation. Part 2: Multidimensional case*, J. Comput. Phys., 257 (2014), pp. 1022–1038.

[28] D. Xiu, *Numerical methods for stochastic computations*, Princeton University Press, Princeton, NJ, 2010. A spectral method approach.

[29] D. Xiu and J. S. Hesthaven, *High-order collocation methods for differential equations with random inputs*, SIAM J. Sci. Comput., 27 (2005), pp. 1118–1139.

[30] D. Xiu and G. E. Karniadakis, *The Wiener-Askey polynomial chaos for stochastic differential equations*, SIAM J. Sci. Comput., 24 (2002), pp. 619–644.

[31] Z. Zhou, *Numerical approximation of the Schrödinger equation with the electromagnetic field by the Hagedorn wave packets*, J. Comput. Phys., 272 (2014), pp. 386–407.

[32] Z. Zhou and G. Russo, *The gaussian wave packets transform for the semi-classical Schrödinger equation with vector potentials*, Communications in Computational Physics, to appear (2018).